TECHNICAL REPORT 3045
September 2016

Beamspace Multiple-Input Multiple-Output Part II: Steerable Antennas in Mobile Ad Hoc Networks

Michael Daly
Jeffery Allen
Marcos Ontiveros
Stephen Aldama

SSC Pacific
San Diego, CA 92152-5001

SSC Pacific
San Diego, California 92152-5001

K. J. Rothenhaus, CAPT, USN
Commanding Officer

C. A. Keeney
Executive Director

ADMINISTRATIVE INFORMATION

The work described in this report was prepared by the Applied Electromagnetics Branch (Code 52250) and the Advanced Electromagnetics Technology Branch (Code 52270) of the System-of-Systems and Platform Design Division (Code 52200), Space and Naval Warfare Systems Center Pacific (SSC Pacific), San Diego, CA. The work was funded through the Office of Naval Research (ONR) In-House Independent Laboratory Research (ILIR) Program and ONR's Expeditionary Maneuver Warfare and Combating Terrorism S&T Department (Code 30).

Released by
D. E. Hurdsman, Head
Applied Electromagnetics
Branch

Under authority of
J. McGee, Head
SoS & Platform Design
Division

SB

EXECUTIVE SUMMARY

Antennas that steer their radiation patterns offer higher gain and interference suppression compared to more omni-directional antennas. It is well known how to synthesize a steerable beam using a phased array or a gimbaled dish antenna. However, manpack or vehicle-mounted Marine Corps antennas must be smaller than a dish and less expensive than a phased array. A class of pattern-reconfigurable antenna including the electronically steerable parasitic array radiator (ESPAR) promises a low form-factor steerable antenna with a single RF input compatible with most Marine Corps radios.

How well these steerable antennas improve throughput in mobile ad hoc networks (MANETs) by limiting intra-network interference is a subject of this report. Additionally to this network analysis, a point-to-point technique known as Beamspace multiple-input multiple-output (MIMO) is studied as a potential solution for enhancing ultra-high frequency (UHF) wireless communications with legacy radios. Beamspace MIMO seeks to emulate a MIMO array's performance by using a switched-beam antenna switching at or faster than the symbol rate. A more extensive background of Beamspace MIMO and a framework for its implementation is given in a prior technical report [1].

This prior technical report documented a system-level throughput increase in point-to-point communications with Beamspace MIMO, provided that a solution existed for transmitting a combination of symbols and beams for a given modulation. As a follow-on to [1], the current report finds that for any higher-order modulation, a solution for practical antenna designs is not likely to exist because most antennas do not synthesize enough spatially differing beams. Thus, Beamspace MIMO is not a practical method of increasing point-to-point throughput.

However, this report finds that steerable antennas may dramatically increase the signal-to-interference and-noise ratio (SINR) at a receiver in a MANET. If all radios in a MANET have steerable antennas and a method of distinguishing a desired signal from interference, simulations and experimental data suggest most radios would experience a significant SINR increase, and consequently, a throughput increase. Simulations of eight radios showed roughly a doubling in throughput by using steerable antennas.

This report first documents the Beamspace MIMO transmission and reception methods following the work done in [1]. Then, it shows that the method for emulating a transmit array of separate antennas is highly unlikely to work for the higher-order modulations that are required for MIMO. Next, the report details the potential throughput increase if antennas in MANETs would optimally steer their beams, through both simulation and over-the-air experiments. Then, a design for a compact ESPAR and control board is given along with antenna measurements. Finally, the report concludes with future ideas toward creating a bolt-on layer compatible with radios currently in service.

CONTENTS

Figures

Tables

1. INTRODUCTION

1.1 OVERVIEW OF MIMO

Most radio systems use a single antenna and transceiver. These systems are referred to as single-input single-output (SISO). Multiple-input multiple-output (MIMO) communication systems use multiple antennas and transceivers at both ends of a wireless link to utilize spatial diversity and increase the spectral efficiency and link reliability. Besides MIMO and SISO, two other systems are single-input multiple-output (SIMO) and multiple-input single-output (MISO). Figure 1 depicts the SISO, SIMO, MISO, and MIMO configurations. The importance of MIMO in the commercial sector has grown to where MIMO is now included in various standards, such as IEEE 802.11n (WIFI), IEEE 802.16 (WIMAX), 3G cellular (HSPA+), and 4G cellular [2].

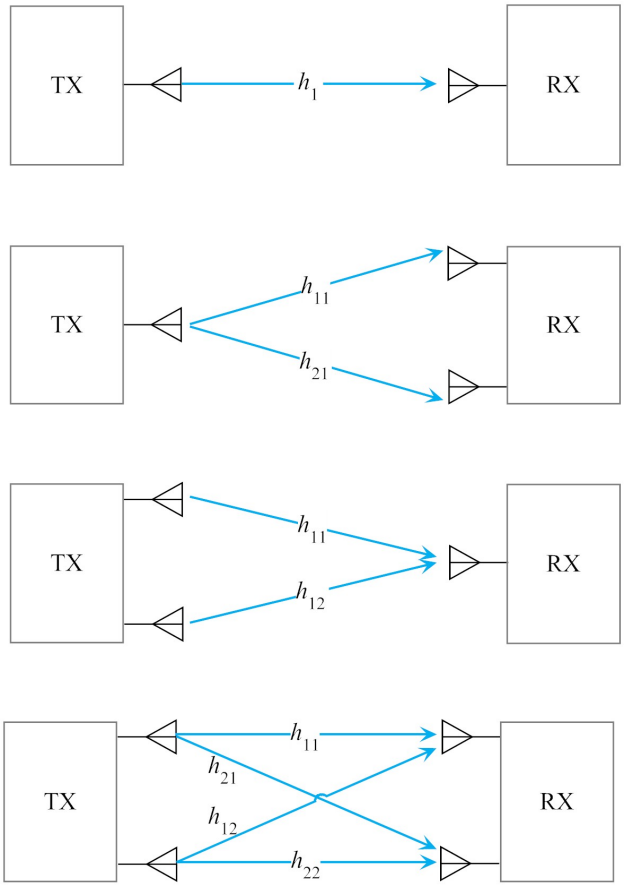

Figure 1. From top to bottom: SISO, SIMO, MISO, and MIMO examples.

1.2 SUMMARY AND PRIOR WORK ON BEAMSPACE MIMO

Beamspace MIMO is a variation of MIMO that, in theory, approaches MIMO capacity using a single transceiver and an electronically steerable directional antenna. Standard MIMO transmits multiple symbol streams simultaneously over each antenna. In contrast, Beamspace MIMO uses a single steerable antenna to transmit multiple symbol streams over each beam pattern, one at a time. The Beamspace MIMO receiver also switches between multiple beam patterns to capture signals from multiple scattering paths. This transmitter and receiver behavior is shown in Figure 2. Therefore, Beamspace MIMO simultaneously

offers increased capacity and backwards compatibility with legacy radios, provided those radios have a Medium Access Control (MAC) layer capable of supporting the protocols developed under this effort. This compatibility offers credible transitions of MIMO technology without procuring new radio systems.

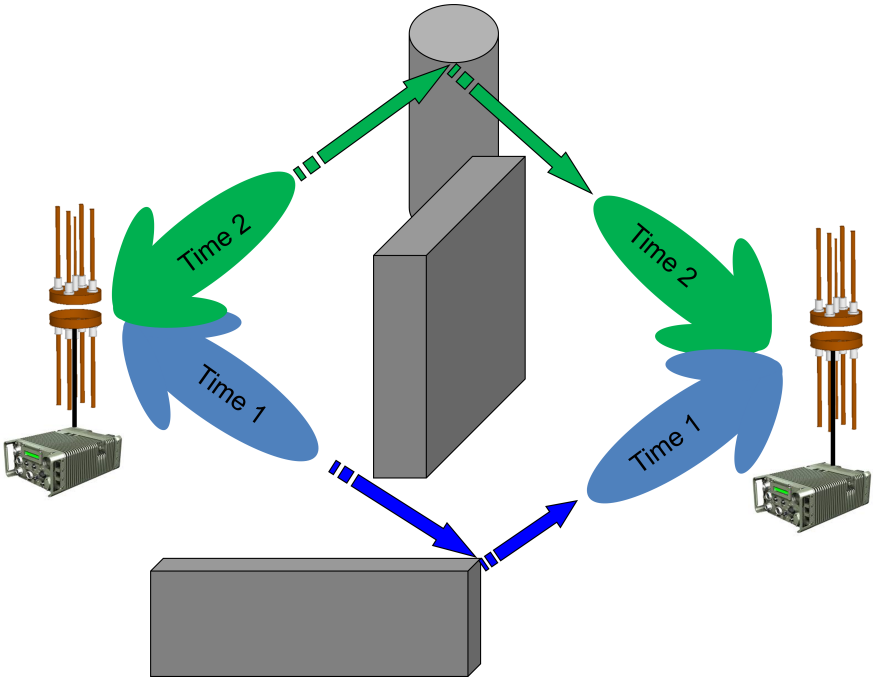

Figure 2. Beamspace MIMO single transceiver solution.

Prior Beamspace MIMO work includes groups in New Zealand [3], Switzerland [4], Japan [5, 6], and Greece [7]. Beamspace MIMO requires electronically steerable antennas. One such antenna is the Electronically Steerable Parasitic Antenna Radiator (ESPAR). The initial applications for ESPARs exploited beam switching for direction finding [6, 7]. Closely allied with direction finding are beam pointing and null steering in a wireless network to maximize signal power and minimize interference [8–10].

The ability to switch beams adds another diversity dimension to the wireless channel. The idea is to use the beams to send independent data streams and appear to a receiver as if the transmitter were an array of spatially-separated antennas. Nomenclatures associated with this approach are aerial diversity [9], pattern diversity [11], spatial multiplexing [12], antenna diversity [3], and beamspace diversity [13]. More detail and a mathematical treatment of Beamspace MIMO is provided in [1].

1.3 OVERVIEW OF BEAMSPACE MIMO IMPLEMENTATION

Prior work on Beamspace MIMO posited implementations assuming an ideal steerable antenna with the ability to synthesize arbitrary patterns. This report describes the framework for choosing beams and symbols to transmit to emulate a multi-element array shown in Figure 3.

MIMO and Beamspace MIMO increase their throughput through spatial multiplexing—sending independent data through different eigenchannels. This necessarily splits the total transmit power among the multiple signals sent over these eigenchannels. In a power-limited regime, there is very little gain from splitting power among spatial eigenchannels and a better strategy is to send all transmit power over the strongest eigenchannel. But in a power-rich regime when there is a good receive signal-to-noise (SNR), spatial multiplexing can greatly increase theoretical throughput [14].

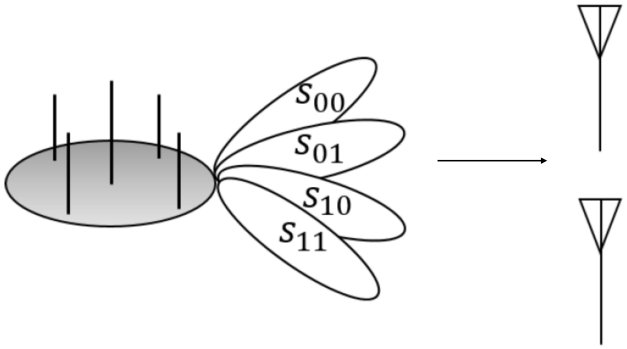

Figure 3. Beamspace MIMO makes a steerable antenna's transmission mathematically equivalent to that of a multi-antenna array.

Higher-order modulations are necessary when the receive SNR increases to transmit near channel capacity. Figure 4 shows that each modulation has a ceiling for the number of bits that can be successfully received per symbol time (channel use), and when the SNR increases to reach that modulation's ceiling, a higher-order modulation should be used to stay near channel capacity (called "BCMIMO capacity" in [1]).

Section 3 details the method to emulate a spatially multiplexing multi-antenna array. Then, the limitations of an antenna with finite patterns to generate higher-order modulations are presented.

1.4 ALTERNATIVE USE OF STEERABLE ANTENNAS IN MANETS

An alternative use for steerable antennas concerns mobile ad hoc networks (MANETs) rather than point-to-point MIMO links. The idea is to steer all nodes' beams in such a way to maximize gain between pairs of radios that want to exchange data, while limiting intra-network interference. Simulations and over-the-air tests compare radios with an ESPAR antenna to radios with omni-directional whip antennas in a MANET, as shown in Figure 5. Results show a significant increase in averagesignal-to-interference-plus-noise ratio (SINR) and throughput in simulations of four transmitter (TX) and receiver (RX) pairs, and measurements of two TX–RX pairs.

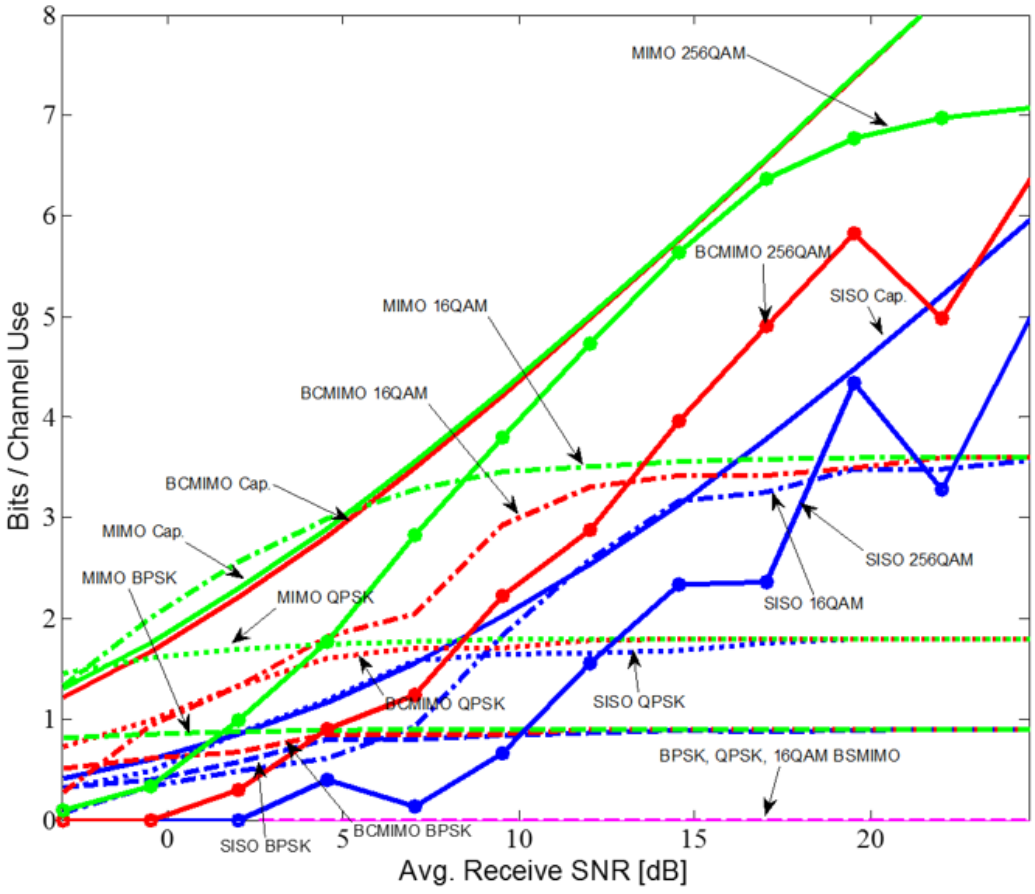

Figure 4. MIMO is only useful at high SNRs, at which higher-order modulation must be used as well to avoid a throughput ceiling.

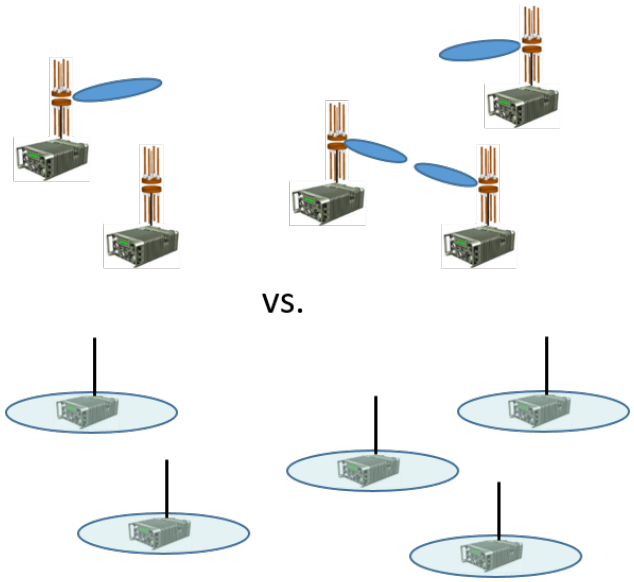

Figure 5. Graphical representation of radio networks equipped with steerable and directional antennas compared to networks carrying only omni-directional antennas.

2. NAVAL RELEVANCE

The U.S. Marine Corps in theater operates with little or no infrastructure, limited or contested spectrum availability, limited power for dismounted soldiers, minimal interoperability between existing legacy equipment, and a high probability of location position intercept. To address these operational drivers, the Office of Naval Research (ONR) is investing in Science and Technology efforts in three main areas: tacti-cal networking, over-the-horizon communications, and small-unit technologies.

This report assesses Beamspace MIMO and steerable antennas in general in the context of MANETs. The Beamspace MIMO approach promises to increase point-to-point throughput over the same bandwidth using the same power as a comparable SISO radio. Steerable antennas promise to increase network throughput by limiting intra-network interference. Increasing network throughput enables several tradeoffs that enhance operational capabilities:

- Increased communication range
- Reduced power
- Reduced antenna footprint compared to MIMO radios.

This report assesses the payoffs of equipping wireless networks with either Beamspace MIMO radios or simply steerable antennas. The focus of the Beamspace MIMO portion is on realizing the Beamspace method using actual ESPAR antennas. The focus of the steerable antennas portion is to produce via simulation an upper bound on network throughput gain. The engineering assessment considers the necessary requirement that the Beamspace MIMO approach must be backwards-compatible with legacy radios. Then, an assessment is made of steerable antennas' ability to improve network throughput. These assessments will determine if steerable antennas and Beamspace MIMO communications deliver a significant shift in operational performance.

3. EVALUATION OF BEAMSPACE MIMO

This section first briefly discusses a framework for an ESPAR antenna to emulate a multi-antenna MIMO array transmitter. More detail of this framework is given in [1]. It is much more straightforward for an ESPAR antenna to emulate a multi-antenna MIMO array on receive: the antenna simply cycles between some or all of its pattern configurations during a symbol period. The second half of this section provides a mathematical explanation of why synthesizing higher-order modulations is not feasible when using the ESPAR antenna in this report.

3.1 BEAMSPACE MIMO ALGORITHM APPROACH

The framework for the transmitter and receiver ESPAR antenna to emulate transmitter and receiver MIMO arrays follows Figure 6. The first graphic shows the physical channel between the ESPAR transmitter on the left and the ESPAR receiver on the right, both dwelling on certain beams that are part of the channel h between them. For simplicity, we will assume single-tap, time-invariant channels and ideal, infinitely fast switching.

The second graphic shows how the receive espar emulates a mimo receiver. The receiver on the right switches between two beams at twice the symbol rate, which creates two channels, h1 and h2, that are each available half of the time. Since the channels are time-invariant, this is equivalent to a two-element fixed antenna array with channels between each element and the transmitter of h1/$\sqrt{2}$ and h2/$\sqrt{2}$. The factor 1/$\sqrt{2}$ scales the signal to half the received power because in reality the beam is only sensing each channel half of the time, which is shown in the third graphic.

The fourth graphic shows how the transmitter ESPAR assigns beams to each modulation symbol. Since the transmitting ESPAR antenna emulates two fixed antennas that send two binary phase shift keying (BPSK) modulated independent streams of data, there are four different combinations that the ESPAR must send (two data streams times two possible symbols per stream). The symbols s_{ij} correspond to the two bits i and j sent at the same time that go on the two spatially-separated data streams. The physical channels between the transmitter and receiver ESPAR are $h_{ij,k}$ where ij corresponds to the two bits sent and also maps to one of the four transmit ESPAR beams, and k corresponds to which of the two beams the receive ESPAR is currently using.

The relationship between the physical channels $h_{ij,k}$, the actual symbols sent s_{ij}, and another set of virtual channels v_{ij} multipllied by the BPSK $+1$ and -1 symbols is given by Equations (1) through (8). A symbol sent through the physical channel $s_{ij}h_{ij,k}$ is equivalent to two BPSK symbols ± 1 sent through virtual channels v_{ab}. That is, the receiver cannot tell if a single ESPAR sent one signal over that physical channel or a two-element array spatially multiplexed two BPSK bit streams over two virtual channels.

$$s_{00}h_{00,1} = +v_{11} + v_{21} \tag{1}$$

$$s_{00}h_{00,2} = +v_{12} + v_{22} \tag{2}$$

$$s_{01}h_{01,1} = +v_{11} - v_{21} \tag{3}$$

$$s_{01}h_{01,2} = +v_{12} - v_{22} \tag{4}$$

$$s_{10}h_{10,1} = -v_{11} + v_{21} \tag{5}$$

$$s_{10}h_{10,2} = -v_{12} + v_{22} \tag{6}$$

$$s_{11}h_{11,1} = -v_{11} - v_{21} \tag{7}$$

$$s_{11}h_{11,2} = -v_{12} - v_{22}. \tag{8}$$

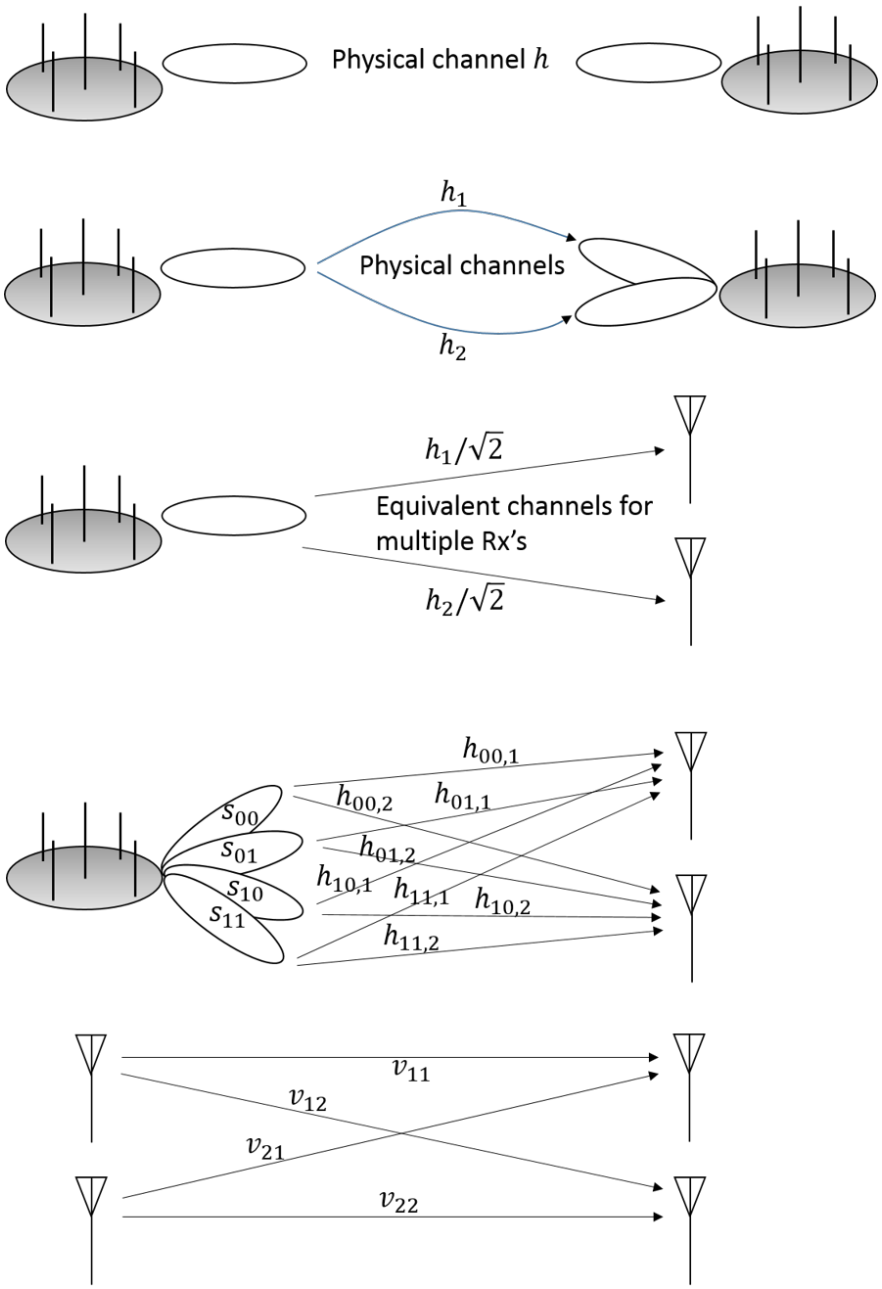

.

Figure 6. Graphical depiction of the framework to convert an ESPAR antenna into a receive array (by cycling between all beams during each symbol period) and a transmit array (by changing the beam and transmitted symbol at the symbol rate). Top: The physical channel between two ESPARs given their choice of beam. Second diagram: the receiver cycles between two beams at twice the symbol rate creating multiple channels to the transmitter. Third diagram: The receiver is equivalent to two antennas with two physical channels to the transmitter with half the channel transfer function power, since the actual receiver dwells on each channel only half the time. Fourth diagram: The transmit array sends four different symbols assigned to each of its four different beams that are switched at the symbol rate. Fifth diagram: To the receiver, the transmitter is equivalent to a two-element array over virtual channels with values related to the physical channels by Equations (1) through (8).

3.2 LIMITATIONS OF FINITE ANTENNA PATTERNS

The preceding section shows the encoding of BPSK onto the antenna patterns to realize Beamspace MIMO. The natural generalization is to encode higher-order modulations onto the antenna patterns to boost throughput. Unfortunately, there are limitations to this encoding. Roughly speaking, the number of antenna patterns must scale with the the number of symbols.

This section details the signal-processing assumptions and shows the impossibility of Beamspace MIMO without "precoding." Essentially, the channel matrix and the symbol matrix must be aligned on their null spaces. A necessary precoder enforcing this alignment is determined. This section closes with two examples showing that this necessary precoder must also limit throughput when the number of antenna patterns does not match the number of symbols.

The canonical BPSK example in the preceding section admits the matrix formulation:

$$\begin{aligned} VX &= \begin{bmatrix} v_{11} & v_{12} \\ v_{21} & v_{22} \end{bmatrix} \begin{bmatrix} 1 & 1 & -1 & -1 \\ 1 & -1 & 1 & -1 \end{bmatrix} \\ &= \begin{bmatrix} h_{00,1} & h_{01,1} & h_{10,1} & h_{11,1} \\ h_{00,2} & h_{01,2} & h_{10,2} & h_{11,2} \end{bmatrix} \begin{bmatrix} b_{00} & 0 & 0 & 0 \\ 0 & b_{01} & 0 & 0 \\ 0 & 0 & b_{10} & 0 \\ 0 & 0 & 0 & b_{11} \end{bmatrix} = HB. \end{aligned}$$

In this setup, the transmitter generates four beams and the receiver emulates two antennas so that the *channel matrix* H is a 2×4 matrix. This channel matrix H arises from the assumption that the transmitter "switches its beam *at* the symbol rate." The receiver is fast switching so that its single physical antenna emulates two receive antennas. However, fast switching at the transmitter spreads the spectrum of the transmitted signal. Consequently, comparisons against a SISO system must allow the SISO system this additional bandwidth or restrict switching to the symbol rate. The transmitter is attempting to emulate two BPSK streams so that the *symbol matrix* X is a 2×4 matrix of ± 1's. Both the symbol matrix X and channel matrix H are given. By assumption, the transmitter broadcasts one Beamspace symbol b_{kl} on one of the four beams. The designer selects a diagonal matrix *beam matrix* B so that the end-to-end system emulates 2×2 MIMO modeled by the *virtual channel matrix* V with nearly full rank.

Generalization to higher-order modulations use the same formalism:

$$VX = HB.$$

Left Side: The *virtual channel matrix* $V \in \mathbb{C}^{N_R \times N_T}$ emulates N_T transmit antennas broadcasting N_R antennas. These receive antennas are the realized from a single fast-switching antenna at the receive site. The *symbol matrix* $X \in \mathbb{C}^{N_T \times N_S}$ lists all symbol vectors in its columns. Thus, VX lists all symbol vectors received through the virtual channel.

Right Side: The *physical channel matrix* $H \in \mathbb{C}^{N_R \times N_B}$ models each beam response at the receive antennas produced by transmitting the beam symbol b_{n_B} ($n_B = 1, \ldots, N_B$) over the physical channel. If the *beam matrix* $B \in \mathbb{C}^{N_B \times N_B}$ is the diagonal of the beam symbols, HB lists all beams received through the physical channel.

Beamspace MIMO Design: A best possible MIMO channel V has all singular values non-zero and equal. Therefore, the design goal seeks a beam matrix B that maximizes the "rank" of the virtual channel matrix V. The "s-rank" is a natural generalization of rank for optimization.

Definition 1 (s-rank) *Let $V \in \mathbb{C}^{M\times N}$ have singular-value decomposition [15] $V = USQ^{\mathsf{H}}$, where $U \in \mathbb{C}^{M\times M}$ is unitary; $Q \in \mathbb{C}^{N\times N}$ is unitary; and $S \in \mathbb{R}^{M\times N}$ has diagonal elements consisting of the singular values $s_1 \geq s_2 \geq \ldots s_K \geq 0$, $K = \min\{M, N\}$. Define the s-rank as the scaled* trace norm*:*

$$\text{s-rank}(V) := \frac{1}{s_1}\sum_{k=1}^{K} s_k.$$

The Beamspace MIMO design are all solutions to the following "naive" optimization problem.

Beamspace MIMO Optimization Given a channel matrix $H \in \mathbb{C}^{N_R\times N_B}$ and a symbol matrix $X \in \mathbb{C}^{N_T\times N_S}$, where $N_B = N_S$, find a diagonal beam matrix B and virtual channel matrix V such that

$$\max\{\text{s-rank}(V) : VX = HB\}.$$

Unfortunately, this optimization problem makes no sense when the constraint equation has no solutions other than the trivial solution.

Example 1 (BPSK) *Suppose X is the BPSK matrix*

$$X = \begin{bmatrix} 1 & 1 & -1 & -1 \\ 1 & -1 & 1 & -1 \end{bmatrix}.$$

X admits the pseudo-inverse:

$$X^{+} = \frac{1}{4}X^{\mathsf{T}} \implies XX^{+} = \begin{bmatrix} 1 & 0 \\ 0 & 1 \end{bmatrix}.$$

Consequently, the solution of $VX = H$ is $V = HX^{+}$. Suppose H is the remaining columns of the 4×4 Hadamard matrix:

$$H = \begin{bmatrix} 1 & 1 & 1 & 1 \\ 1 & -1 & -1 & 1 \end{bmatrix}$$

Then

$$V = HX^{+} = \begin{bmatrix} 0 & 0 \\ 0 & 0 \end{bmatrix}$$

substituting this solution back into $VX = H$ gives the result

$$VX = \begin{bmatrix} 0 & 0 & 0 & 0 \\ 0 & 0 & 0 & 0 \end{bmatrix} \neq \begin{bmatrix} 1 & 1 & 1 & 1 \\ 1 & -1 & -1 & 1 \end{bmatrix} = H.$$

Roughly speaking, $VX = HB$ can only be solved when X and HB have null spaces that are in alignment.

Definition 2 *Let $A \in \mathbb{C}^{M\times N}$. The* null space *or "kernel" of A is*

$$\mathcal{N}(A) := \{\mathbf{x} \in \mathbb{C}^N : A\mathbf{x} = \mathbf{0}\}.$$

The co-kernel *of A is the orthogonal complement:*

$$\mathcal{N}(A)^{\perp} := \{\mathbf{x} \in \mathbb{C}^N : \mathbf{y}^{\mathsf{H}}\mathbf{x} = 0\}.$$

Lemma 1 *Let $H \in \mathbb{C}^{M\times N}$ and $X \in \mathbb{C}^{M\times N}$. Assume*

A-1 $M \leq N$

A-2 *X is full rank:* $\mathrm{rank}(X) = M$.

A-3 $\mathcal{N}(X) \supseteq \mathcal{N}(H)$

Then $VX = H$ if and only if $V = HX^{+}$.

Proof: Decompose $\mathbb{C}^N = \mathcal{N}(X)^{\perp} \oplus \mathcal{N}(X)$. A-1 and A-2 force

$$M = \dim(\mathcal{N}(X)^{\perp}); \quad L = \dim(\mathcal{N}(X));.$$

Factor X and H over this decomposition:

$$X = \begin{matrix} \\ M \end{matrix} \begin{matrix} \begin{matrix} M & L \end{matrix} \\ \begin{bmatrix} X_1 & \mathbf{0} \end{bmatrix} \end{matrix}; \quad H = \begin{matrix} \\ M \end{matrix} \begin{matrix} \begin{matrix} M & L \end{matrix} \\ \begin{bmatrix} H_1 & H_2 \end{bmatrix} \end{matrix},$$

where X_1 is invertible. A-3 forces $H_2 = \mathbf{0}$. Then

$$\begin{aligned} VX = H &\iff V\begin{bmatrix} X_1 & \mathbf{0} \end{bmatrix} = \begin{bmatrix} H_1 & \mathbf{0} \end{bmatrix} \\ &\iff VX_1 = H_1 \\ &\iff V = H_1 X_1^{-1} \\ &\iff V = \begin{bmatrix} H_1 & \mathbf{0} \end{bmatrix} \begin{bmatrix} X_1^{-1} \\ \mathbf{0} \end{bmatrix} \\ &\iff V = HX^{+}. \end{aligned}$$

///

Lemma 1 explains Example 1—If the null space of X does not contain in the null space of H, the matrix H_2 is non-zero and multiplication by X^{+} destroys this channel information:

$$V = HX^{+} = \begin{bmatrix} H_1 & H_2 \end{bmatrix} \begin{bmatrix} X_1^{-1} \\ \mathbf{0} \end{bmatrix} = H_1 X_1^{-1}.$$

Indeed, H_2 is lost when V is substituted into the original equation:

$$VX = H_1 X_1^{-1} \begin{bmatrix} X_1 & \mathbf{0} \end{bmatrix} = \begin{bmatrix} H_1 & \mathbf{0} \end{bmatrix} \neq \begin{bmatrix} H_1 & H_2 \end{bmatrix}.$$

Lemma 1 shows that $VX = HB$ can only be solved when X is full rank and its null space contains the null space of HB: $\mathcal{N}(X) \supseteq \mathcal{N}(HB)$. The channel matrix H is given by the real world whereas the symbol matrix X is determined by the modulation scheme. Therefore, X must be modified to enforce the null-space alignment. This modification requires the projection onto the co-kernel of HB.

For simplicity, assume also that the channel matrix H is also full rank and the beam matrix B zeros no beams. Then the SVD of HB has the form

$$HB = U \begin{bmatrix} S & \mathbf{0} \end{bmatrix} \begin{bmatrix} W_1^{\mathsf{H}} \\ W_2^{\mathsf{H}} \end{bmatrix},$$

where $S > 0$ is $N_R \times N_R$. The columns of W_2 are an orthogonal basis for the null space of HB: The columns of W_1 are an orthogonal basis for the co-kernel of HB:

$$\mathcal{N}(X)^{\perp} = W_1 \mathbb{C}^{N_R}$$

and an orthogonal projection onto the co-kernel is

$$P = W_1 W_1^{\mathsf{H}}.$$

If the new symbol matrix is XP, then

$$\mathcal{N}(XP) \supseteq \mathcal{N}(P) = \mathcal{N}(H).$$

Therefore, the virtual Beamspace MIMO design takes the following form:

VBS-MIMO Optimization Given a channel matrix $H \in \mathbb{C}^{N_R \times N_B}$ and a symbol matrix $X \in \mathbb{C}^{N_T \times N_S}$, where $N_B = N_S$. Assume that H is full rank and there are more beams than transmitters. Let $P \in \mathbb{C}^{N_B \times N_B}$ any orthogonal projection onto the co-kernel of HB: Find a diagonal beam symbol matrix B and virtual channel matrix V such that

$$\max\{\text{s-rank}(V) : VXP = HB\},$$

that is, Beamspace MIMO must adapt its symbols to the channel. Consequently, the projection matrix P can be considered a variant of precoding.

Example 2 (VBS-MIMO: 2×4 **BPSK)** *This example tests the feasibility of VBS-MIMO using the BPSK example in Section 3.2:*

- *Four-beam transmitter*
- *Two emulated receive antennas*
- *Gaussian channel matrix.*

Figure 7 displays the average performance of this VBS-MIMO approach. The upper panel reports the channel rank for the Gaussian channel. The middle panel plots the ratio of the channel ranks to show the gain in rank:

$$\rho(V, H) = \frac{\text{s-rank}(V)}{\text{s-rank}(H)}.$$

The bottom panel plots the distribution of this ratio. The virtual channel approach gains approximately 30% in rank when operating over the Gaussian channel.

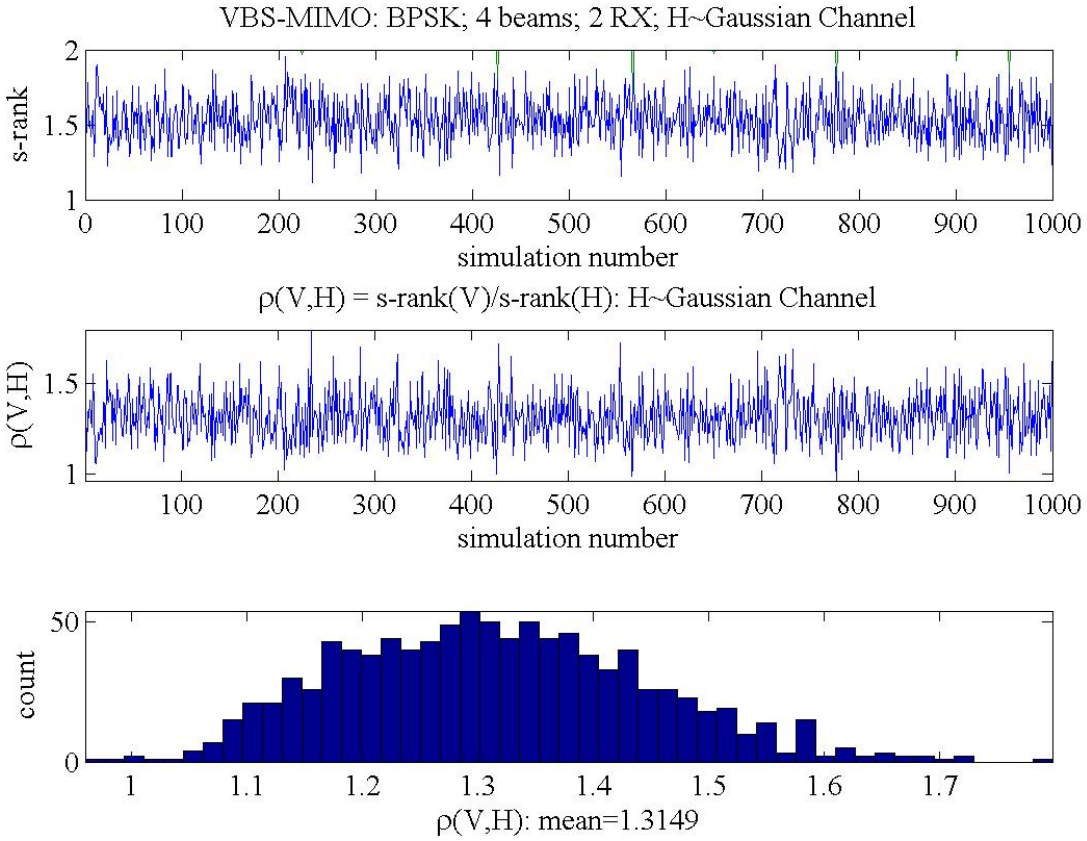

Figure 7. VBS-MIMO: TX employs four beams; RX emulates two antennas.

Example 3 (VBS-MIMO: 2×8 **BPSK)** *This example extends VBS-MIMO using BPSK with eight beams:*

- *Eight-beam transmitter*
- *Two emulated receive antennas*
- *Gaussian channel matrix.*

Figure 8 has the same form as the preceding example. The bottom panel shows the "bottom line": increas-ing the number of beams does not boost the channel rank over the four-beam case.

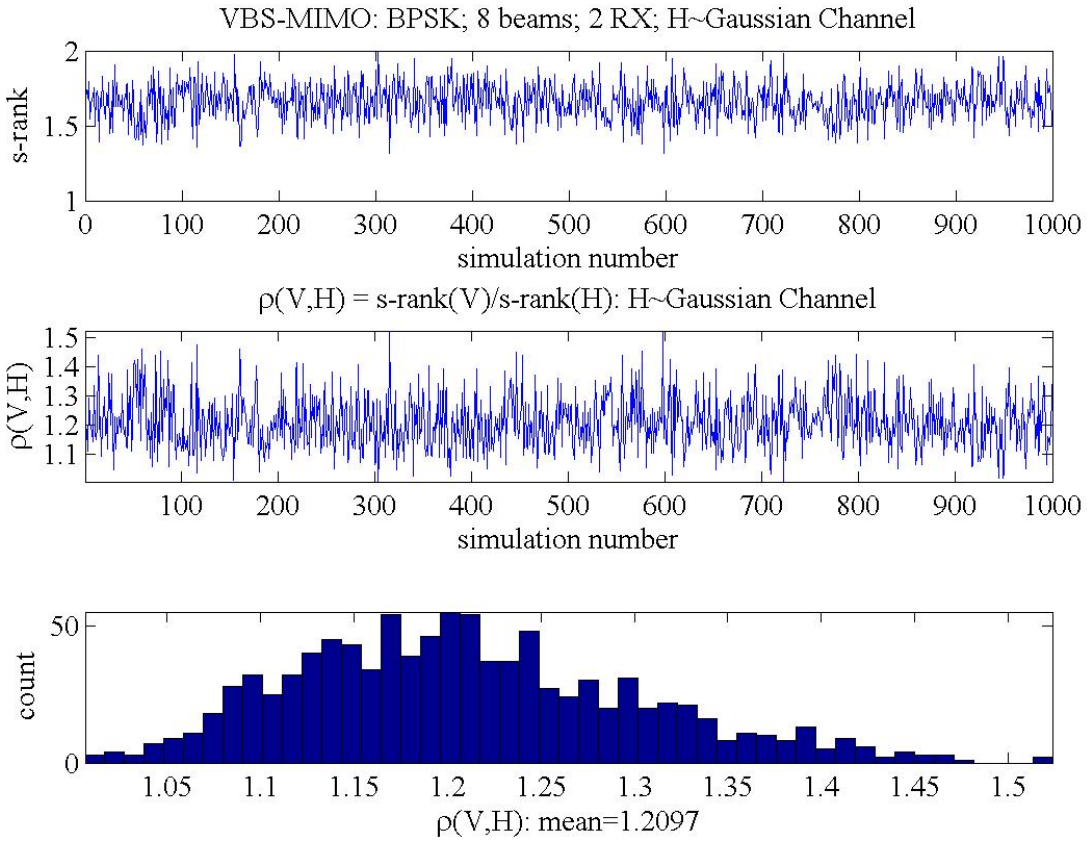

Figure 8. VBS-MIMO: TX employs eight beams; RX emulates two antennas.

4. STEERABLE ANTENNAS IN MANETS

Steerable antennas promise to lower intra-network interference in MANETs by focusing transmitters' radiation toward the desired receivers and not toward other receivers. At these receivers, steerable beams will reject more of the radiation from other sources while increasing the gain of the desired signal. This section reviews prior work on steerable antennas in MANETs and then presents new simulation and measurement results. SINR is used as a proxy for throughput since it is independent of the communications protocol. This work does not attempt to develop a new MAC protocol that is better suited to steerable antennas. Rather, we assume the MAC protocol of a legacy radio will remain the same with a bolt-on layer that includes the steerable antenna adjusting its beam based on radio feedback. If SINR feedback is not available from a legacy radio, Section 6.2 gives some ideas on how a bolt-on layer could steer the antenna beam with no radio feedback.

4.1 PRIOR WORK

Prior work applying steerable antennas to MANETs has focused on developing MAC protocols to leverage radiation pattern directionality. A 2012 review paper cataloged 38 MAC protocols that took antenna beamforming into account [16]. Most of these protocols are for MANETs and are random access as opposed to synchronized access. The challenges of including steerable antennas in MANETs include:

- Deafness (a node does not hear a request to send)
- Hidden terminals (more often than with omni-directional antennas, another node will be unknown to a pair of nodes that talk over it)
- Head-of-line blocking (the protocol waits for a particular node's response that is not received because it steered its beam away from the querying node)
- Range under-utilization (a protocol requires a node to use an omni-directional pattern for some part when a directional pattern would achieve longer range)
- MAC-layer capture (a node does not do anything intelligent with its radiation pattern while idle).

A 2005 survey of directional antenna-based MACs listed other challenges such as "cost, system complexity, and practicality of fast steerable directional antennas" [17].

Over the past 15 years, there have been several highly cited papers on directional MAC protocols. In [18], a CSMA-based protocol was shown to offer 28% to 118% improvement in throughput over omni-directional antennas. The paper stressed that link power control is essential. In [19], another simulated directional MAC protocol found a throughput increase over omni-directional antennas.

A rare over-the-air test of a MAC protocol was presented in [20] using a switched array of directional antennas on a vehicle. One conclusion was that performance increases do not necessarily come from higher gain but rather from a good front-to-back ratio. The front-to-back ratio was the dominant factor because the over-the-air test was an interference-dominated rather than noise-dominated environment. The importance of beam nulling rather than steering solely for maximum gain of the desired signal is also shown by results presented in this report in Section 4.4, when sometimes a better SINR was achieved by steering beams away from the desired other node because interference was decreased more than signal power.

4.2 RAY TRACING SIMULATIONS

This section presents a MANET of omni-directional vs. directional antennas using channels simulated from a ray tracing code. A model of part of Rosslyn, Virginia, was used in the ray tracing code NEC-BSC [21] to approximate channels between four transmitter–receiver pairs. All channels were simulated at 300 MHz. The four transmitters were at fixed locations shown by red dots in Figure 9. The receivers were randomly placed anywhere in the figure, except 30 m from a transmitter or inside a building. Narrowband communications was assumed, so single-tap channels were calculated between all transmitter and all re-ceivers.

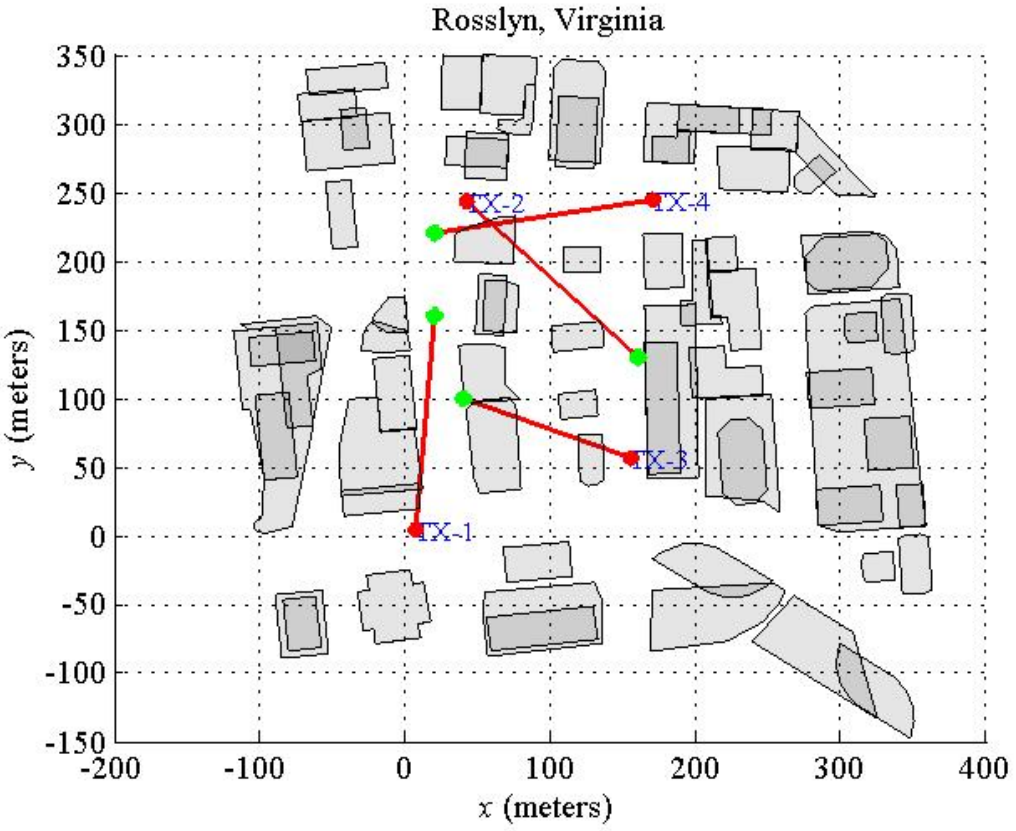

Figure 9. Top view of a 3-D urban environment: street-level transmitter locations are fixed; street-level receiver locations are random; links are the lines connecting a transmitter to a receiver.

The throughput upper bound for a TX–RX pair is a function of SINR. We assume a noise power of -130 dBW and that each transmitter's power is 1 W. The whip patterns and ESPAR patterns are normalized to an average absolute gain of one. The SINR on link $l = 1, 2, 3, 4$ is computed as

$$\gamma_l = \frac{g_{ll} p_{T,l}}{p_N + \sum_{m \neq l} g_{lm} p_{T,m}},$$

where $p_{T,l}$ is the transmitter's power on link l, $p_{N,l}$ is the noise power at the input to the receiver on link l, and g_{lm} is the channel magnitude squared between transmitter m and receiver l. Implicit in this "flat" channel channel is the narrowband assumption: the carrier frequency is $f_C = 300$ MHz; the bandwidth is $f_B = 25$ kHz. all transmitters broadcast unit power: $p_{T,l} = 0$ dBW. Likewise, all receivers are subject to the same "flat" additive noise at $p_{N,l} = -130$ dBW.

Figure 10a is an estimate of the SINR distribution when both the transmitters and receiver are equipped with vertical whips. The street-level transmitter locations are fixed; The street-level receiver locations are drawn at random uniformly scattered throughput the 3-D region at the street level but constrained to be 30 meters away from any transmitter and exterior to any building. The histogram shows the SINR for 1,000 random networks.

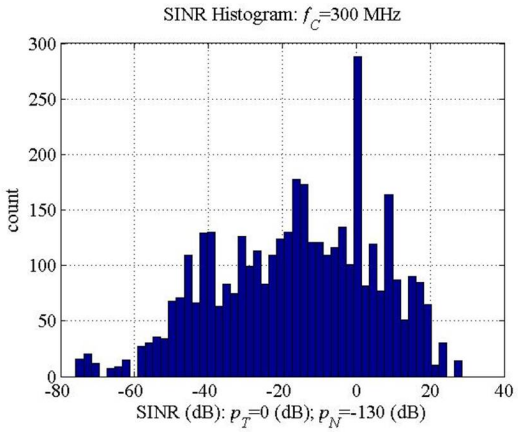

(a) Histogram of the SINR in the urban environment; transmitters and receivers are equipped with vertical whips; Transmitter's power: $p_{T,l} = 1$ W; Noise Power: $p_{N,l} = -130$ dBW.

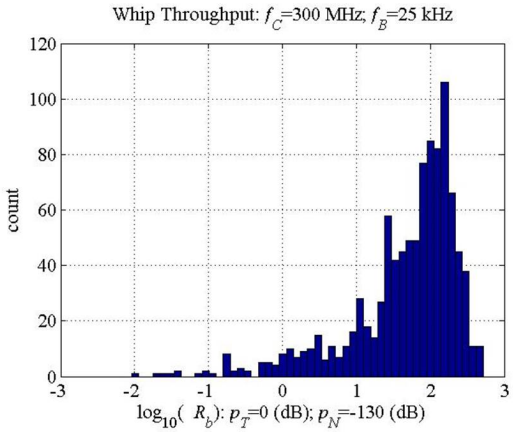

(b) Histogram of the throughput in the urban environment; transmitters and receivers are equipped with vertical whips; Transmitter's power: $p_{T,l} = 1$ W; Noise Power: $p_{N,l} = -130$ dBW.

Figure 10. Simulated SINR and network throughput when antennas are whips.

The SINR provides an upper bound on throughput under the following assumptions:

- Interference is modeled as independent white Gaussian noise
- Channels are static
- Channels are perfectly known at each receiver.

An upper bound on the throughput of the lth link is

$$R_{b,l} \leq f_B \ \log_2(1+\gamma_l); \quad \text{[bps]}.$$

Network throughput bounded as

$$R_b \leq f_B \ \sum_{l=1}^{4} \log_2(1+\gamma_l); \quad \text{[bps]}.$$

Figure 10b is an estimate of the distribution of the throughput. There is a mean around 100 kbps but a long tail.

For fixed transmitter and receivers, the gain matrix changes when the transmitters and receivers use a vertical whip or the directional ESPAR antennas. The next two plots report on the SINR and throughput when both transmitters and receivers are equipped with an ESPAR that produces four beams. In this simulation, the beam directions are aligned with the streets and the beams point $\pm X$ and $\pm Y$. The four

transmitters and four receivers generate $4^8 = 65,536$ beam combinations gain matrices. A network "genie" is assumed to exist. This genie selects beam combinations that maximize total throughput. Figure 11a presents such a genie-aided estimate of the SINR subject to the following limitation: the genie only looked over 10,000 beam combinations in this simulation rather than the entire 65,000. Although the SINR is actually a low estimate, comparison with the SINR produced by the whips shows the genie-aided network migrates the SINR to the upper values. This shift in performance is reflecting in the throughput. Figure 11b presents an estimate of the distribution of the throughput. In comparison to the whips, the mean has shifted to roughly 200 kbps while the tail of this distribution has been shorted.

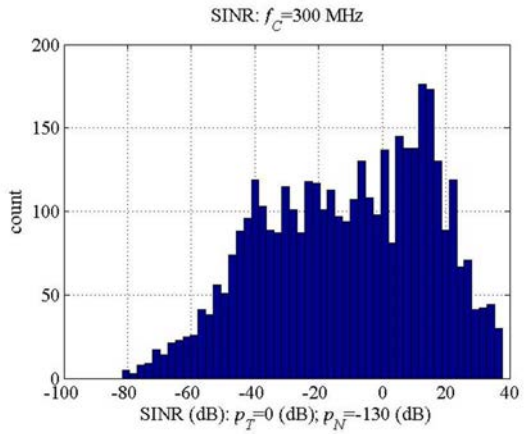

(a) Histogram of the SINR in the urban environment delivered by genie-aided pattern selection; transmitters and receivers are equipped with ESPAR $\pm X, \pm Y$; Transmitter's power: $p_{T,l} = 1$ W; Noise Power: $p_{N,l} = -130$ dBW.

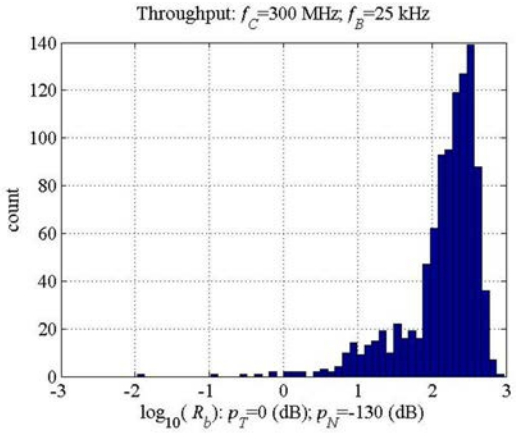

(b) Histogram of the throughput in the urban environment delivered by genie-aided pattern selection; transmitters and receivers are equipped with ESPAR $\pm X, \pm Y$; Transmitter's power: $p_{T,l} = 1$ W; Noise Power: $p_{N,l} = -130$ dBW.

Figure 11. Simulated SINR and network throughput when antennas are ESPARs.

Table 1 quantifies this performance shift. For both the mean and the median, network throughput approximately doubles when the network is equipped with the genie-aided pattern selection. This pattern selection also forces closer alignment of the mean and median because the low end of the throughput tail has been shorted.

Table 1. Network throughput performance shifts delivered by genie-aided pattern selection over whips.

Antenna	Mean (kbps)	Median (kbps)
Whip	98	76
Pattern selection	211	194

The value of this simulation is that the performance shift that the ESPAR selection is quantified. In an urban environment with lots of multipath, these bounds shows an adroit selection of the beams doubles the throughput. However, the "cost-of-business" requires an approximation of the genie-aided pattern selection. Basic questions are as follows:

- *Is doubling the network throughput large enough to survive implementation?*
- *Does doubling the network throughput scale with network size?*
- *What distributed power selection algorithms deliver throughput near the genie-aided selection?*

The next section undertakes a hardware development supporting first steps toward distributed pattern selection.

4.1 SDR MEASUREMENT SETUP

To verify the trends reported in simulation, two TX–RX pairs were created with either quarter-wavelength whip or ESPAR antennas. Each TX or RX includes a laptop connected via Ethernet® to a software-defined radio (SDR). The RF daughter board in the TX SDRs generates a BPSK-modulated waveform centered at 300 MHz. In the case of whip antennas, the RF port is simply connected to the whip antenna. In the case of the ESPAR antenna, the RF port of the radio is connected to the driven element of the ESPAR. There is also a digital input/output (I/O) board connected by USB to the laptop to generate the appropriate voltages for the ESPAR control board to switch to one of the four beams. Eight output voltages and ground from the digital I/O board connect to a socket on the exterior of the ESPAR control board. A diagram of this connection is shown in Figure 12.

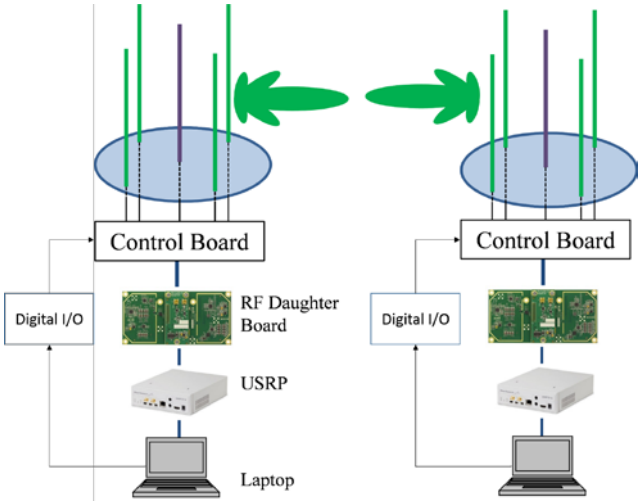

Figure 12. Integration of ESPAR antenna with an SDR.

The laptops run LabVIEW codes to send or receive waveforms. The waveforms generated by the transmitters are BPSK-modulated orthogonal codes. The two codes used are part of the set of Global Positioning System (GPS) Coarse/Acquisition codes (codes 2 and 3). These are Gold codes 1023 bits long that have an autocorrelation close to a delta function. Additionally, the two codes have a nearly zero cross-correlation for all alignments. Nearly zero cross correlation allows the signals from two transmitters to be received simultaneously and the power from each transmitter calculated independently. Let the upsampled BPSK sequence from TX 1 be denoted by $s1[n]$ and the sequence from TX 2 denoted by $s2[n]$. Each BPSK sequence is transmitted at a symbol rate of 400 kSps and is upsampled to two samples per symbol and raised root cosine filtered. Each sequence is $N = 2046$ samples long.

The receivers make a raw received power measurement as a check on the power measurement through correlation with a code. Let the received signal be given by $r[n]$. The raw power is then

$$P_{raw} = \frac{\sum_{n=0}^{N-1} |r[n]|^2}{N}. \tag{9}$$

The power from transmitter b is calculated from the received samples using the following equation:

$$P_b = \frac{\max\limits_n \left(\sum\limits_{k=0}^{N-1} s_b^*[k] r[n+k] \right)^2}{N \sum\limits_{k=0}^{N-1} |s_b[k]|^2} \,. \tag{10}$$

If the received signal is a copy of the signal transmitted by TX b scaled by a complex channel h, the received power calculated by the correlation method reduces to

$$P_b = \frac{|h|^2}{N} \sum_{k=0}^{N-1} |s_b[k]|^2 \,.$$

Neglecting noise (which is explained in Section 4.4), this will be equal to the raw power calculation in Equation (9) with $r[n] = hs_b[n]$.

If the received signal is from the other TX c where $b \neq c$, the correlation

$$\max_n \left(\sum_{k=0}^{N-1} s_b^*[k] s_c[n+k] \right)$$

is approximately zero.

To quantify correlation parameters, the transmitter radios were placed 7 ft away from the receiver radios down a hallway, with the TXs and RXs both spaced 4 ft apart. All radios were connected to whip antennas. One transmitter was turned on at a time and the power from each receiver recorded using the correlation method. The powers were calculated using both orthogonal codes. Thus, there are eight measurements in all (two receivers $\times$ two power correlations per transmitter $\times$ two transmitters). The difference between the correlation power measurements using the correct code vs. the code not sent was 25.4 dB on average.

To test the accuracy of measuring received power using (10), first, both receivers' noise floors were measured with no antenna connected and were within 0.3 dB of each other. No power meter was used to calibrate the actual received power based on numerical values and all power measurements discussed are relative power. Then, both receivers measured power when one TX was on, so the raw power and the power from a correlation should be equal. The power from Equation (9) was within 2 dB of the power computed from Equation (10) for both radios.

Finally, both transmitters were turned on and correlations to measure power were again made on both receivers using both codes. The power measurements of each respective transmitter with both transmitters on were within 0.3 dB of the power measurements when the power was on for only one of the transmitters. From these tests, we conclude that the correlation method is an accurate way to determine the received power from both transmitters that are simultaneously transmitting at the same frequency.

4.4 SDR EXPERIMENTS

In all of the experiments presented, the minimum power received from one of the transmitters is at least 14 dB greater than the noise-plus-interference level when an antenna is plugged into a radio but no transmitter is on. Usually, the power received is 10s of dBs greater. We conclude that the environments measured are interference-dominated rather than noise floor-dominated.

That the noise can be neglected also allows for a difference in gain between the two antenna types. Ideally, the average gain of the ESPARs and whips would be the same if SINR is the metric. In practice, the average gain of the whips was 2.5 dB less than the average gain of the ESPARs. Because noise is negligible in the SINR calculation and if the gains of all ESPARs are assumed to be approximately the same (the measured gains of two of the ESPARs were approximately identical) and the gains of the whips are approximately the same, then the gains cancel in the numerator and denominator of the SINR. SINR is then determined by channel and pattern shape, the important parameters in this experiment, instead of radiation efficiency.

The first experiment is shown in Figure 13. Either two whips or two ESPARs serve as transmitters down a long hallway. They are spaced 4 ft apart and the hallway width is 6.5 ft and ceiling height just over 10 ft. Down the hallway 55 ft are two other whips or ESPARs serving as receivers. ESPAR beams are positioned so that Beam 1 of each transmitter faces left in Figure 13, and Beam 1 of each receiver faces right. Beams are numbered counter-clockwise looking down at the antenna.

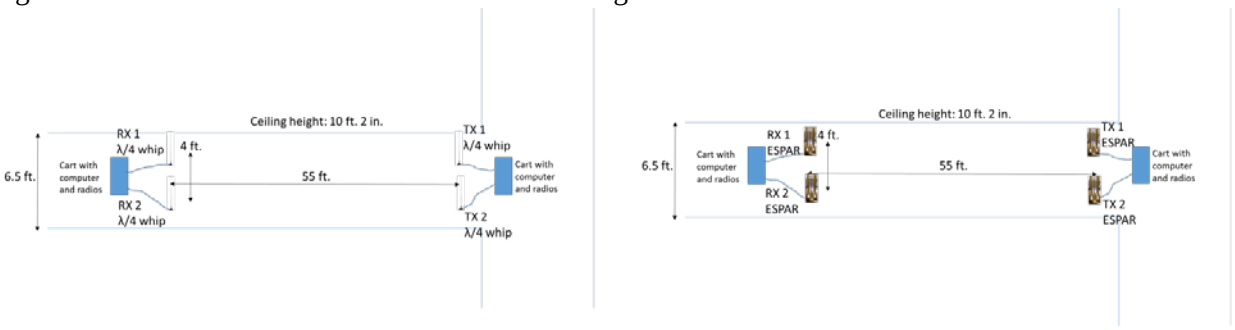

Figure 13. Experimental setup of ESPAR and whip antennas for two pair interference test down a long straight hallway.

Table 2 shows the resulting SINRs measured when the intention is for TX 1 to send to RX 1 and TX 2 to RX 2, and the experiment is repeated with the intention for TX 1 to transmit to RX 2 and TX 2 to RX 1. For the whip antennas, the SINR from TX b to RX a, $b \neq a$, will always be the opposite of the SINR from TX b to RX b. This is because the receiver always sees the same power from both transmitters, and is treating one as signal and the other as interference, and other noise is negligible.

The ESPAR antenna beams were switched until a good SINR was found for both experiments. Beams were switched by hand rather than exhaustively testing all 44 combinations. The beams used for each TX–RX pair are recorded in Table 2. Even though every combination of beams was not tested, good enough combinations were found by hand so that the SINR from each ESPAR TX–RX pair was always positive. The average SINR achieved by the ESPAR RXs was 8.2 dB higher on average than that that achieved by the whip RXs.

Figure 14 shows the next experiment where there is no longer a line-of-sight path from TX to RX. The ESPAR Beam 1 of the TX antennas faces right and Beam 1 of the RX antennas faces down. Slightly dif- ferent best beams were found for the ESPARs than in the previous experiment. It is interesting to note that the best beams for the transmitters were the same in both experiments, and these occurred with the beams of each transmitter facing each other and pointed toward the middle of the hall. All SINRs for the whips and the best beam combinations found for ESPARs are shown in Table 3. Although the difference in aver- age SINR was not as great as the line-of-sight test down the hallway, the ESPAR RXs achieved an average SINR 4.5 dB higher than the whip RXs.

Table 2. SINR for two pairs of whip or ESPAR antennas transmitting simultaneously down a long hallway shown in Figure 13.

Experiment	TX 1 → RX 1 and TX 2 → RX 2 (dB)	ESPAR Beams Used
Whip SINR TX 1 → RX 1	-1.1	
ESPAR SINR TX 1 → RX 1	12.5	2 → 3
Whip SINR TX 2 → RX 2	-6.0	
ESPAR SINR TX 2 → RX 2	7.2	4 → 3
Experiment	TX 1 → RX 2 and TX 2 → RX 1 (dB)	
Whip SINR TX 1 → RX 2	1.1	
ESPAR SINR TX 2 → RX 1	3.6	2 → 1
Whip SINR TX 2 → RX 1	6.0	
ESPAR SINR TX 1 → RX 2	12.2	4 → 1
Summary		
Average Whip SINR	2.0	
Average ESPAR SINR	10.2	
ESPAR SINR improvement	8.2	

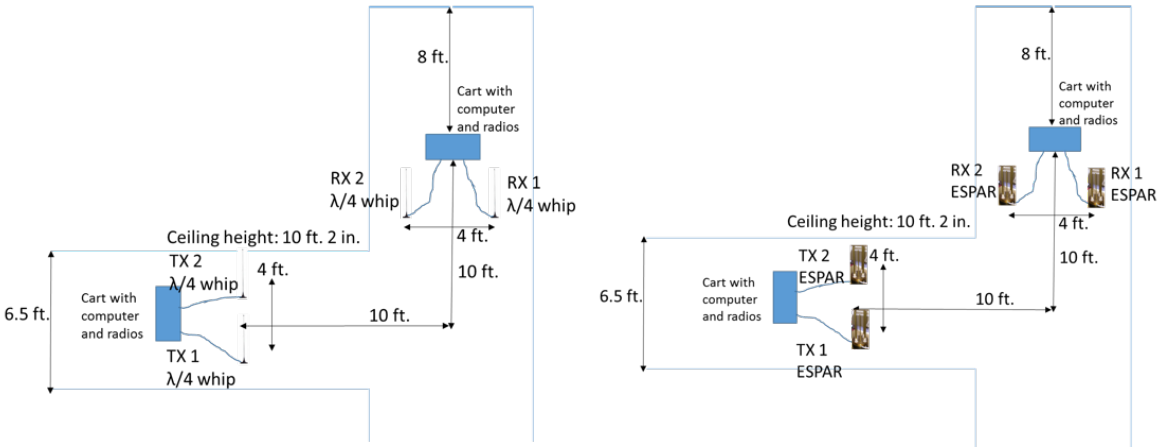

Figure 14. Experimental setup of ESPAR and whip antennas for two pair interference test around a corner of a hallway.

The final test depicted in Figure 15 uses two pair of ESPARs or whips outdoors, roughly 50 ft from the nearest scattering building. The ground is made of asphalt with metal mesh. The transmitters are spaced 48 ft. from the receivers. Beam 1 of the receivers faces down and Beam 1 of the transmitters faces up, when viewed from above in the figure.

Table 2 shows the resulting SINRs for whips and ESPARs. The best combination of ESPAR beams when TX *b* was intended for RX *b* was for the transmitter beams to face the receivers and the receiver beams to face away from the transmitters. Pointing the receiver beams in the opposite direction greatly reduced received power, but in the interference-limited environment, slightly improved SINR. When TX *b* was intended for RX *a*, with $a, b \neq a$, then the best combination was for all four beams to face forward toward the opposite pair of antennas. Since there are less paths rays can take between transmitters and receivers than the indoors cases, the ESPARs have less options from which they might find a better configuration to mitigate interference. Thus, the SINR improvement from the ESPARs is the least of all scenarios, with only a 1.5-dB improvement on average over using whip antennas.

Table 3. SINR for two pairs of whip or ESPAR antennas transmitting simultaneously around a hallway corner shown in Figure 14.

Experiment	TX 1 → RX 1 and TX 2 → RX 2 (dB)	ESPAR Beams Used
Whip SINR TX 1 → RX 1	-0.2	
ESPAR SINR TX 1 → RX 1	7.0	2 → 1
Whip SINR TX 2 → RX 2	5.5	
ESPAR SINR TX 2 → RX 2	9.2	4 → 3
Experiment	TX 1 → RX 2 and TX 2 → RX 1 (dB)	
Whip SINR TX 1 → RX 2	0.2	
ESPAR SINR TX 2 → RX 1	2.1	2 → 3
Whip SINR TX 2 → RX 1	-5.5	
ESPAR SINR TX 1 → RX 2	1.4	4 → 1
Summary		
Average Whip SINR Average ESPAR SINR	1.6	
ESPAR SINR improvement	4.5	

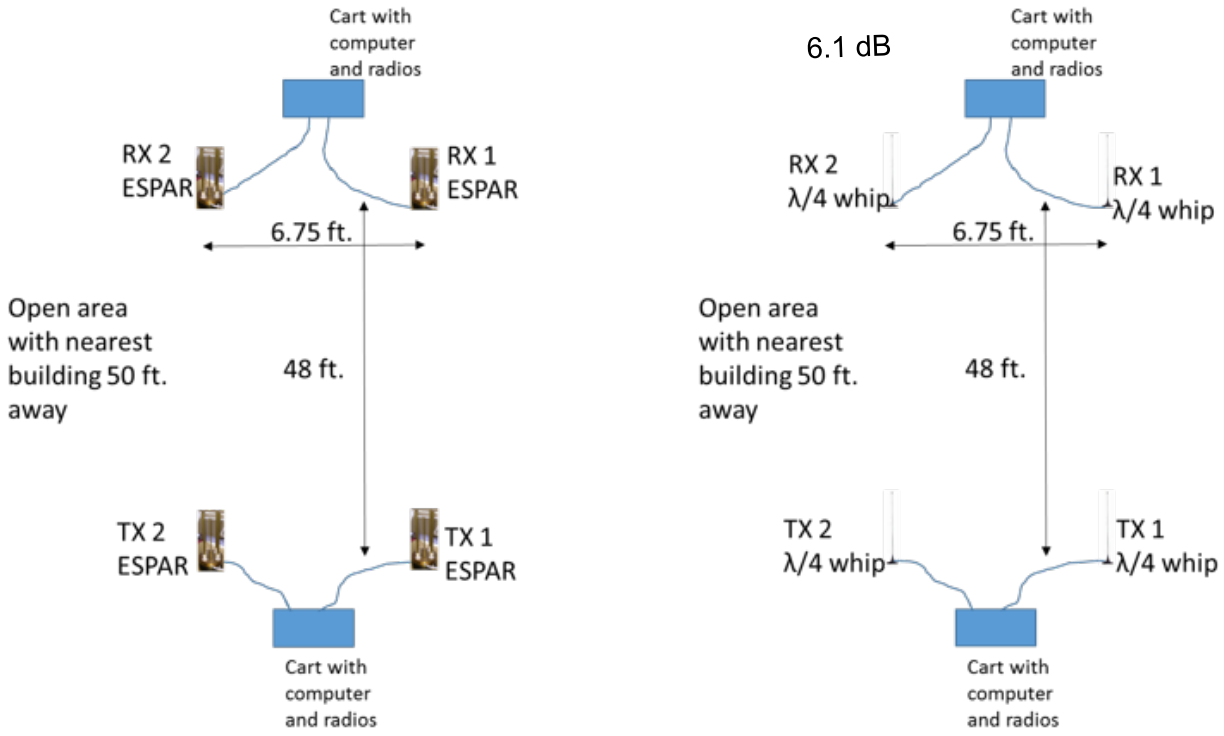

Figure 15. Experimental setup of ESPAR and whip antennas for two pair interference test outdoors in an open paved area.

Table 4. SINR for two pairs of whip or ESPAR antennas transmitting simultaneously in an open outdoors paved area shown in Figure 15.

Experiment	TX 1 → RX 1 and TX 2 → RX 2 (dB)	ESPAR Beams Used
Whip SINR TX 1 → RX 1	-5.2	
ESPAR SINR TX 1 → RX 1	-1.8	1 → 3
Whip SINR TX 2 → RX 2	-4.4	
ESPAR SINR TX 2 → RX 2	0.3	1 → 3
Experiment	TX 1 → RX 2 and TX 2 → RX 1 (dB)	
Whip SINR TX 1 → RX 2	5.2	
ESPAR SINR TX 2 → RX 1	6.8	1 → 1
Whip SINR TX 2 → RX 1	4.4	
ESPAR SINR TX 1 → RX 2	4.8	1 → 1
Summary		
Average Whip SINR	2.3	
Average ESPAR SINR	3.8	
ESPAR SINR improvement	1.5	

5. ESPAR FINAL DESIGN

An ESPAR was chosen as the candidate antenna in this report's simulations and measurements because of its compatibility with single-feed legacy radios and low cost. An ESPAR consists of a center antenna element surrounded by parasitic antenna elements. The spacing between the center element and parasitic elements is typically 0.25λ, where λ is the free-space wavelength. Only the center element is connected to a transceiver. The ESPAR antenna generates different radiation patterns by loading the parasitic elements with different reactance values. Varactors are used in most ESPAR designs to produce the desired patterns. Because of their low complexity, ESPARs are inexpensive.

5.1 ANTENNA DRIVEN AND PARASITIC ELEMENTS

An ESPAR antenna was developed that has a reduced inter-element spacing of $4\times$ less than conventional designs. For a ultra-high frequency (UHF) wavelength of 1 m, the inter-element spacing of the antenna reduces from 0.25 to 0.065 m. A photograph of the ESPAR is shown in Figure 16. The antenna diameter is slightly larger due to the collar where the electronics are held.

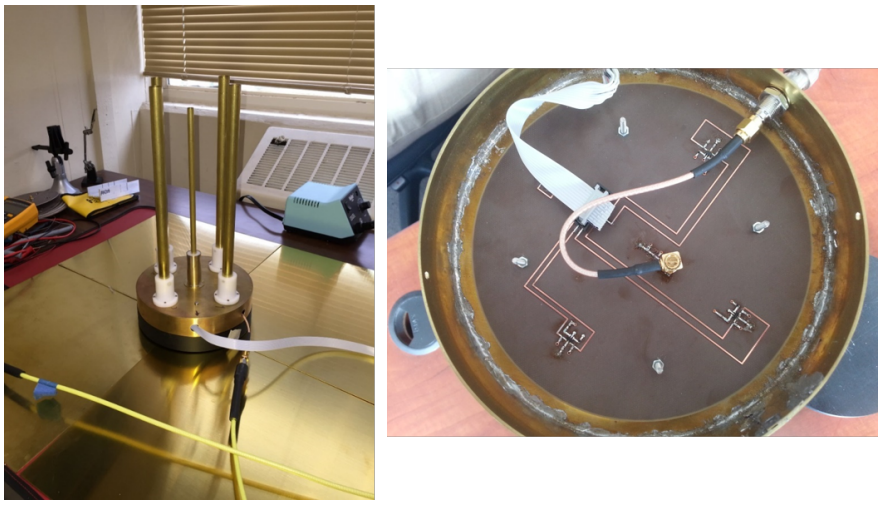

Figure 16. ESPAR final design and control board.

5.2 SWITCHES, PARASITIC LOADING, AND CONTROL BOARD

The antenna is capable of four beams directed 90° apart in azimuth. The antenna uses Hittite HMC 545 single-pole double-throw (SPDT) RF switches to switch to each beam pattern by adjusting the loads on the parasitic elements. These switches are chosen because of their fast switching capability. Each parasitic antenna element can behave as either a reflector or director depending on the parasitic load that is presented to it via the RF switch. Circuit simulations showed that the values needed at the parasitic elements were nearly identical to open and short loads at the desired frequency. A 1 MΩ and an ideal short were connected to each SPDT switch, as shown in Figure 17.

The control board is a printed circuit board (PCB) that serves as the interface for the digital I/O from the radio to the RF switches connected to the parasitic elements, and for the RF port to the radiating antenna element via a matching circuit.

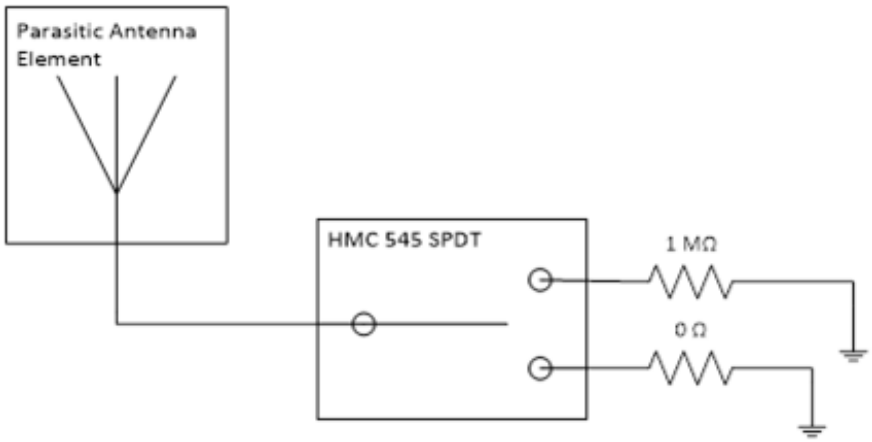

Figure 17. Parasitic antenna element with RF switch circuit.

5.3 IMPEDANCE AND RADIATION PATTERN MEASUREMENTS

The ESPAR is designed for a center frequency of 300 MHz and its return loss is shown in Figure 18. A symmetrical $S_{11} < -10$ dB bandwidth of 10 MHz around this center frequency is sufficient for the waveforms transmitted in Beamspace MIMO tests.

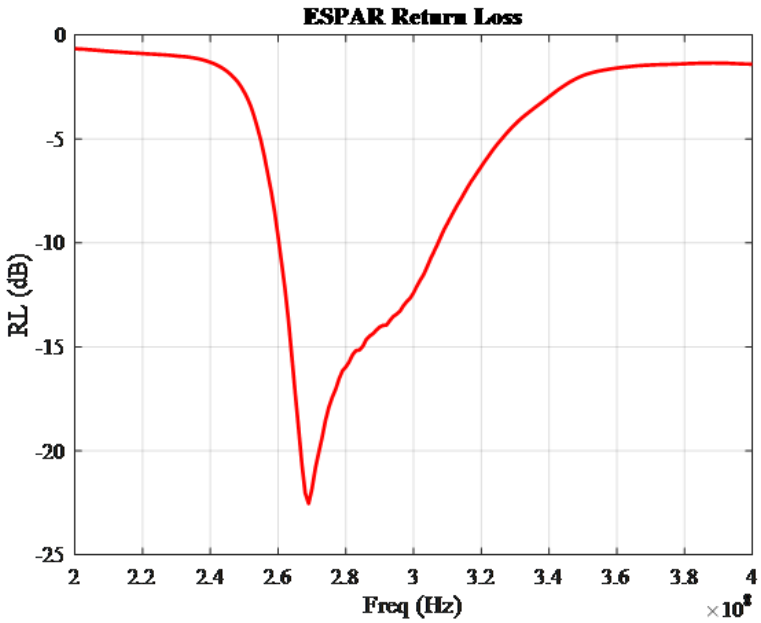

Figure 18. The return loss of one of the ESPAR antennas designed for 300 MHz.

Figure 19 shows the measured realized gain of an ESPAR antenna at 5° elevation at 300 MHz. The antenna was measured on an outdoor pattern range at the Space and Naval Warfare Center Pacific in San Diego, Califonia. The 5° elevation is very close to ground level and is near the lowest elevation angles that can be measured on this pattern range. The beams formed by different choices of parasitic loads are nearly sym-metric. The maximum gain of the antenna is approximately 8.5 dBi.

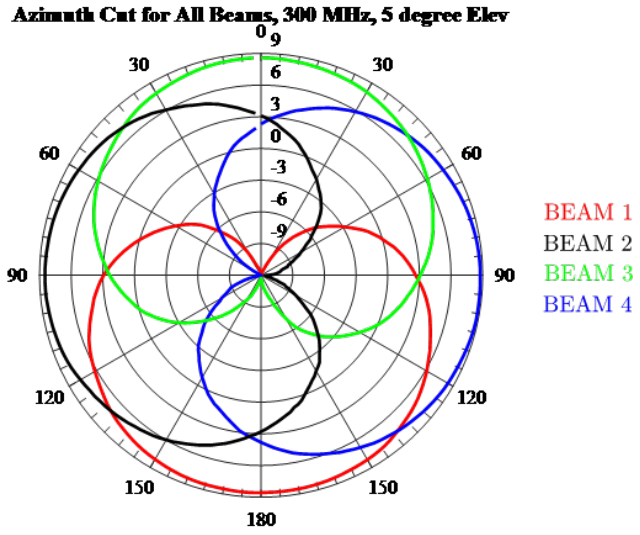

Figure 19. An azimuthal cut of the measured radiation patterns of an ESPAR antenna at 5° elevation and 300 MHz.

6. SUMMARY AND FUTURE WORK

6.1 PROJECT SUMMARY

This report proposed an implementation for Beamspace MIMO that is compatible with existing antenna designs such as ESPARs. With modulations of greater cardinality than BPSK that are necessary for efficient communications, it was found that the ESPAR antenna was unable to synthesize even two spatially multiplexed data streams. Beamspace MIMO was concluded to be impractical for this antenna design. However, using this ESPAR in a MANET was shown via simulation and measurement to improve the average SINR seen at all receivers. Thus, the use of this steerable antenna should improve average net-work throughput over using omni-directional antennas.

6.2 FUTURE WORK

The ESPAR antenna is intended to be part of a bolt-on layer for existing fielded military radios. Besides connecting to the RF port of the radio, the antenna beam-steering circuitry must be operated either internally or by voltages input from the radio. Future investigation will determine what type of feedback such as SINR or received signal strength indicator (RSSI) is available from common UHF radios such as the Harris PRC-117G.

Ideally, a candidate radio has an SINR output that could go to a microprocessor in the bolt-on layer. The microprocessor would direct beam-steering periodically to search for a beam achieving a better SINR or when the SINR drops below a threshold. SINR is more desirable than RSSI because the main job of a steerable antenna is to limit intra-network interference. If RSSI is the only feedback available from a radio, there may still be some benefit to a distributed beam algorithm that seeks either to maximize or minimize received power. An initial investigation of such a benefit is presented next. As a side note, if a radio does not output RSSI, this can be measured in the bolt-on layer.

The same ray tracing simulation environment of Section 4.2 is used for this investigation, with the same four fixed TX and four RX nodes placed randomly. The choice of beams by the TX and RX nodes in the simulation was entirely individual without other nodes' coordination. In one iteration, one of the eight nodes was randomly selected to adjust its beam to one of three criteria: maximize received power, minimize received power, or randomly adjust. It is assumed the RX nodes emit some kind of training data so the TX nodes can also steer based on the received power from all four RX nodes. Then another node was randomly selected and the same process repeated for the next iteration. When the goal was to maximize or minimize received power, the nodes converged on a solution for a given set of positions in about 20 iterations. When the simulation was rerun with nodes started at different random beams, the solution converged to the same set of beams. To be safe that all nodes had converged to a solution, 100 iterations were run for maximizing or minimizing received power.

It is evident from Figure 20 that links using either antenna type see a wide range of SINRs due to channel variation. However, the average SINR seen by a receiver with an ESPAR antenna is nearly 5 dB higher than the SINR seen by a receiver with a whip antenna. This is despite the fact that a RX node may steer toward the highest power coming from a TX node that is one of the three interferers and not the desired TX node. The histogram and SINR difference was after 10,000 simulations. This number of simulations was assumed sufficient because in all three cases presented in this section (Figures 20, 21, and 22), the average SINR at receivers with whip antennas was 9.1, 9.1, and 9.3 dB, respectively. These numbers should be the same, as nothing changed when rerunning the whip case.

The results when the ESPAR antennas steer to minimize the RSSI are shown in Figure 21. Now the ESPAR antennas perform worse than the whip antennas on average.

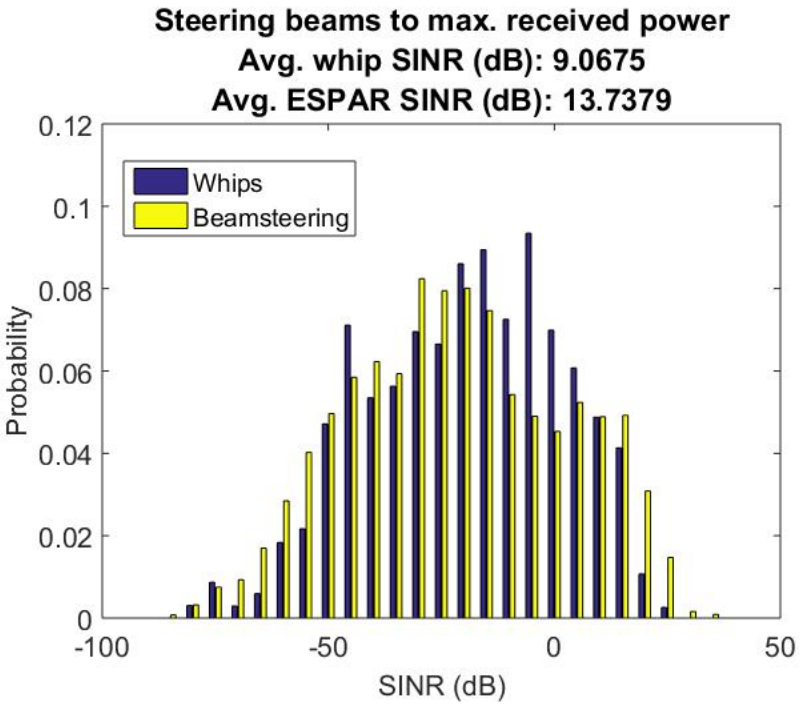

Figure 20. Histograms of the SINRs achieved by four TX–RX pairs having either whip or ESPAR radiation patterns randomly placed in the scattering environment of Figure 9. The ESPARs choose the one of their four beams with the highest receive power, not attempting to discern if the power is interference or the desired signal.

Finally, the results when all eight ESPAR antennas randomly choose a beam are shown in Figure 22. It is curious that this slightly outperforms on average using omni-directional whip antennas, and this result requires additional investigation.

These results indicate that some performance benefit is possible even if the bolt-on layer has no feedback from the radio. But based on the over-the-air test results using SDRs that could adjust the beam based on SINR, an increase in radios' SINRs, and consequently, network throughput, is expected if SINR can be fed to the antenna. The availability legacy radio feedback will drive further development of a bolt-on layer.

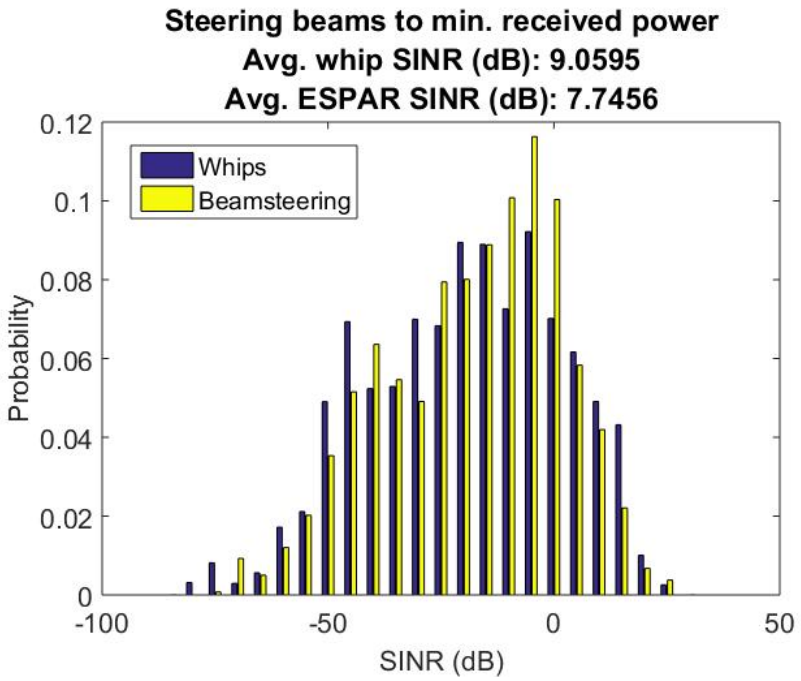

Figure 21. Histograms of the SINRs achieved by four TX–RX pairs having either whip or ESPAR radiation patterns randomly placed in the scattering environment of Figure 9. The ESPARs choose the one of their four beams with the lowest receive power, not attempting to discern if the power is interference or the desired signal.

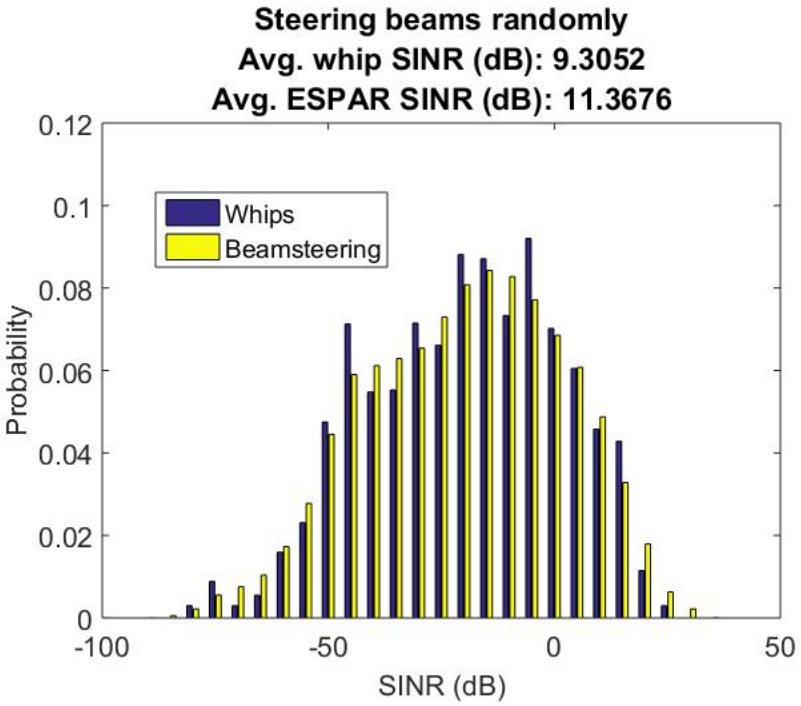

Figure 22. Histograms of the SINRs achieved by four TX–RX pairs having either whip or ESPAR radiation patterns randomly placed in the scattering environment of Figure 9. The ESPARs randomly choose one of their four possible beams.

7. LIST OF ACRONYMS

- BPSK: Binary phase shift keying
- ESPAR: Electrically steerable parasitic array radiator
- GPS: Global Positioning System
- I/O: Input/output
- MAC: Medium access control
- MANET: Mobile ad hoc network
- MIMO: Multiple input multiple output
- ONR: Office of Naval Research
- PCB: Printed circuit board
- RSSI: Received signal strength indicator
- RF: Radio frequency
- RX: Receiver
- SDR: Software-defined radio
- SIMO: Single input multiple output
- SINR: Signal to interference and noise ratio
- SISO: Single input single output
- SNR: Signal-to-noise ratio
- SPDT: Single-pole double-throw
- TX: Transmitter
- UHF: Ultra-high frequency
- USRP: Universal software radio peripheral

REFERENCES

1. Arceo, D., J. Allen, M. Ontiveros, J. James, and M. Daly. 2015. "Beamspace MIMO Phase I: Simulation Study." Technical Report 2078 (May). Space and Naval Warfare Systems Center Pacific (SSC Pacific). San Diego, California.
2. Sibille, A., C. Oestges, and A. Zanella. 2010. *MIMO: From Theory to Implementation*. Academic Press, Burlington, MA.
3. Vaughan, R. 1999. "Switched Parasitic Elements for Antenna Diversity," *IEEE Transactions on Antennas and Propagation*, vol. 47, no. 2, pp. 399–405.
4. Yousefbeiki, M., and J. Perruisseau-Carrier. 2014. "Towards Compact and Frequency-Tunable Antenna Solutions for MIMO Transmission with a Single RF Chain," *IEEE Transactions on Antennas and Propagation*, vol. 62, pp. 1065–1073.
5. Ohira, T., and K. Iigusa, K. 2004. "Electronically Steerable Parasitic Array Radiator Antenna." *Electronics and Communications in Japan (Part II: Electronics)*, vol. 87, no. 10, pp. 25–45.
6. Taillefer, E., A. Hirata, and T. Ohira. 2005. "Direction-of-arrival Estimation using Radiation Power Pattern with an ESPAR antenna." *IEEE Transactions on Antennas and Propagation*, vol. 53, no. 2, pp. 678–684.
7. Plapous, C., J. Cheng, E. Taillefer, A. Hirata, and T. Ohira. 2004. "Reactance Domain MUSIC Algorithm for Electronically Steerable Parasitic Array Radiator." *IEEE Transactions on Antennas and Propagation*, vol. 52, no. 12, pp. 3257–3264.
8. Sun, C., A. Hirata, T. Ohira, and N. C. Karmakar. 2004. "Fast Beamforming of Electronically Steerable Parasitic Array Radiator Antennas: Theory and Experiment." *IEEE Transactions on Antennas and Propagation*, vol. 52, no.7, pp. 1819–1832.
9. Iigusa, K., H. Harada, and S. Kato. 2010. "Proposal and Design of a Slim Electronically Steerable Parasitic Array Radiator Antenna in the 2.4-GHz Band," *Wireless Personal Communications*, vol. 52, no. 1, pp. 43–55.
10. Ando, A. 2002. "Analysis of ESPAR Antennas in Indoor Multi-path Environments for Wireless Ad-hoc Network Systems." *IEEE Wireless Communications and Networking Conference (WCNC) Record, Volume 2* (pp. 586–591). March 17–21, Orlando, FL. IEEE.
11. Kumar, S., J. Chamberland, and G. Huff, G. 2013. "Reconfigurable Antennas, Preemptive Switching and Virtual Channel Management under Partial Observations." *2013 U.S. National Committee of URSI National Radio Science Meeting (USNC-URSI NRSM)* (pp. 1–1). January 9–15, Boulder, CO. IEEE.
12. Alrabadi, O. N., A. Kalis, C. B. Papadias, and A. G. Kanatas. 2008. "Spatial Multiplexing by De-composing the Far-field of a Compact ESPAR Antenna." *IEEE 19th International Symposium on Personal, Indoor and Mobile Radio Communications (PIMRC)* (pp. 1–5), September 15–18, Paris, France. IEEE.
13. Alrabadi, O. N., J. Perruisseau-Carrier, and A. Kalis. 2012. "MIMO Transmission using a Single RF Source: Theory and Antenna Design," *IEEE Transactions on Antennas and Propagation*, vol. 60, no. 2, pp. 654–664.
14. Daly, M., Ontiveros, M., Allen, J., Buchanan, K., and Arceo, D. (2015). "Measured 2 × 2 MIMO UHF channels in an urban environment." In *2015 IEEE International Symposium on Antennas and Propagation & USNC/URSI National Radio Science Meeting*, pp. 296–297, IEEE.
15. Stewart, G. W. 1973. *Introduction to Matrix Computations*. Academic Press. 1st ed. New York, NY.

16. Bazan, O., and M. Jaseemuddin. 2012. “A Survey on MAC Protocols for Wireless Adhoc Networks with Beamforming Antennas,” *IEEE Communications Surveys & Tutorials*, vol. 14, no. 2, pp. 216–239.

17. Akyildiz, I. F., and X. Wang. 2005. “A Survey on Wireless Mesh Networks,” *IEEE Communications Magazine*, vol. 43, no. 9, pp. S23–S30.

18. Ramanathan, R. 2001. “On the Performance of Ad Hoc Networks with Beamforming Antennas.” *Proceedings of the 2nd ACM International Symposium on Mobile Ad Hoc Networking & Computing* (pp. 95–105). October 4–5, Long Beach, CA. ACM.

19. Choudhury, R. R., X. Yang, R. Ramanathan, and N. H. Vaidya. 2002. “Using Directional Antennas for Medium Access Control in Ad Hoc Networks.” *Proceedings of the 8th Annual International Conference on Mobile Computing and Networking* (pp. 59–70). September 23–28, Atlanta, GA. ACM.

20. Ramanathan, R., J. Redi, J., C. Santivanez, D. Wiggins, and S. Polit. 2005. “Ad Hoc Networking with Directional Antennas: A Complete System Solution,” *IEEE Journal on Selected Areas in Communications*, vol. 23, no. 3, pp. 496–506.

21. Marhefka, R. J., and W. D. Burnside. 1982. *Numerical Electromagnetic Code Basic Scattering Code (Version 2), Part I: User’s Manual*. The Ohio State University ElectroScience Laboratory, Columbus, OH.

REPORT DOCUMENTATION PAGE

Form Approved
OMB No. 0704-01-0188

PLEASE DO NOT RETURN YOUR FORM TO THE ABOVE ADDRESS.

1. REPORT DATE *(DD-MM-YYYY)*	2. REPORT TYPE	3. DATES COVERED *(From - To)*
September 2016	Final	

4. TITLE AND SUBTITLE

Beamspace Multiple-Input Multiple-Output
Part II: Steerable Antennas in Mobile Ad Hoc Networks

5a. CONTRACT NUMBER

5b. GRANT NUMBER

5c. PROGRAM ELEMENT NUMBER

6. AUTHORS

Michael Daly
Jeffery Allen
Marcos Ontiveros
Stephen Aldama

5d. PROJECT NUMBER

5e. TASK NUMBER

5f. WORK UNIT NUMBER

7. PERFORMING ORGANIZATION NAME(S) AND ADDRESS(ES)

SSC Pacific
53560 Hull Street
San Diego, CA 92152–5001

8. PERFORMING ORGANIZATION REPORT NUMBER

TR 3045

9. SPONSORING/MONITORING AGENCY NAME(S) AND ADDRESS(ES)

Office of Naval Research
One Liberty Center
875 N. Randolph Street, Suite 1425
Arlington, VA 22203-1995

SSC Pacific
In-House Independent Labortory Research Program - Applied Research
53560 Hull Street
San Diego, CA 92152-5001

10. SPONSOR/MONITOR'S ACRONYM(S)

ONR; SSC Pacific

11. SPONSOR/MONITOR'S REPORT NUMBER(S)

12. DISTRIBUTION/AVAILABILITY STATEMENT

Approved for public release.

13. SUPPLEMENTARY NOTES

14. ABSTRACT

This report finds that steerable antennas may dramatically increase the signal-to-interference-and-noise ratio (SINR) at a receiver in a mobile ad hoc network (MANET). If all radios in a MANET have steerable antennas and a method of distinguishing a desired signal from interference, simulations and experimental data suggest most radios would experience a significant SINR increase, and consequently, a throughput increase. Simulations of eight radios showed roughly a doubling in throughput by using steerable antennas.

The report first documents the Beamspace multiple-input multiple-output (MIMO) transmission and reception methods following the work done in a 2015 Space and Naval Warfare Systems Center Pacific technical report. Then, it shows that the method for emulating a transmit array of separate antennas is highly unlikely to work for the higher-order modulations that are required for MIMO. Next, the report details the potential throughput increase if antennas in MANETs would optimally steer their beams, through both simulation and over-the-air experiments. Then, a design for a compact electronically steerable parasitic array radiator (ESPAR) and control board is given along with antenna measurements. Finally, the report concludes with future ideas toward creating a bolt-on layer compatible with radios currently in service.

15. SUBJECT TERMS

Mission Area: Communications
antenna systems design; signal-to-interference-and-noise ratio; mobile ad hoc network; electronically steerable parasitic array radiator; Beamspace multiple-input multiple-output; channel modeling; end-to-end systems; radio-frequency switches

16. SECURITY CLASSIFICATION OF:			17. LIMITATION OF ABSTRACT	18. NUMBER OF PAGES	19a. NAME OF RESPONSIBLE PERSON
a. REPORT	b. ABSTRACT	c. THIS PAGE			Michael Daly
U	U	U	U	42	19B. TELEPHONE NUMBER *(Include area code)* (619) 553-2666

INITIAL DISTRIBUTION

84300	Library	(1)
85300	Archive/Stock	(1)
52250	M. Daly	(1)
52250	J. Allen	(1)
52270	M. Ontiveros	(1)
52270	S. Aldama	(1)

Defense Technical Information Center
Fort Belvoir, VA 22060–6218 (1)

Approved for public release.

SSC Pacific
San Diego, CA 92152-5001